Journal of Electrical Engineering and Automation (ISSN: 2582-3051)
www.irojournals.com/iroeea/

DPC of Cross-compensated Virtual Flux Double Switch Table

He Liu[1], Wang Ya-Jun[2]

[1]Power Electronics and Electric Drives, Liaoning University of Technology, China
[2]Professor, Department of Electronic and Information Engineering, Liaoning University of Technology, China

E-mail: [1]1447781864@qq.com

Abstract

Aiming at the problems of large power ripple, high harmonic components and DC bias on the AC side of the three-phase voltage rectifier Direct Power Control (DPC), as well as the shortcomings of the voltage output of the DC side busbar, the direct power control method of the cross-compensated virtual flux double switch meter has been proposed. The virtual flux can realize the sensorless mode on the input side of the circuit to reduce the high harmonic, even if the first-order low-pass filter is used to replace the integration region, there is still some error. On this basis, the two filters are connected in parallel for virtual flux compensation, and then the voltage vector is selected according to the instantaneous power change, and the sector is re-divided with the voltage as the control vector, and two independent switching state tables are designed. The cross-compensated virtual flux double-switch meter DPC is simulated and compared with the traditional DPC waveform, and the experimental results show that the cross-compensated virtual flux double-switch meter DPC strategy can effectively reduce the proportion of harmonic content, control power fluctuations, improve DC bias, has fast tracking effect, stabilize output voltage, and control active and reactive power flexibly. The three-phase voltage rectifier circuit occupies an important position for the pre-rectifier part of the charging power supply of electric vehicles, and the rectifier circuit that can stabilize the output DC voltage cannot only extend its service life for the charging power supply, but also reduce harmonic pollution.

Keywords: Three phase voltage source PWM rectifier, DPC, virtual flux linkage, switch meter

DOI: https://doi.org/10.36548/jeea.2021.4.005
Received: 24.02.2022, received in revised form: 08.03.2022, accepted: 22.03.2022, published: 04.04.2022

1. Introduction

PWM rectifiers can convert variable currents into direct current, realize the "ecological conversion" of electrical energy [1], and require direct current in new energy fields such as wind power generation, synchronous motors, and electric vehicle charging power sources, so PWM rectifiers between power equipment and public power grids are essential, and the control of three-phase voltage PWM rectifiers is also crucial. Its commonly used controls are sliding mode control, direct current control, direct power control and so on. Synovial control is a sliding mode control theory that makes the whole system move on the state trajectory set in advance, although the uncertainty of the entire system is overcome, but the state trajectory is difficult to slide strictly towards the balance point, which will cause the output to jitter [2]. Direct current control is controlled by a dual closed-loop method of voltage outer loop and current inner loop, but when the load changes, the load power changes ahead of the DC bus response, resulting in an imbalance of input and output energy [3]. Direct power control (DPC) also uses dual-loop control, except that the inner loop is changed to power, and then the high-power factor is achieved through the switching meter and the DC output voltage is stabilized [4]. Compared with the first two controls, the algorithm of the DPC strategy is simpler and the response speed is faster, so the DPCs of the three-phase voltage PWM rectifier are studied in depth.

The literature [5-6] introduces the virtual flux directional direct power control, adding a virtual flux on the basis of DPC, which can not only reduce the number of sensor devices, but also reduce the total harmonic distortion rate of the system, but there will still be DC bias errors. The literature [7] explains that the zero vector in the switching state table not only has little effect on the control of reactive power, but also causes large power ripples. The application of virtual flux-based DPC in voltage source type HVDC (VSC-HVDC) is proposed, and the relationship between switching meters and power is not discussed in depth, and power fluctuations still exist. Aiming at the above problems, a virtual flux is introduced in the three-phase circuit, and the integration region is replaced by a parallel compensation low-pass filter, and the sector of the traditional DPC is subdivided, and the active power and reactive power are controlled separately by a double-switch table. The improved DPC control not only eliminates the network side voltage sensor, reduces the cost, but also has good stability, has a good suppression effect on harmonics, and at the same time, realizes the reasonable adjustment of P and Q, and reduces the oscillation of DC side power and DC side voltage when the load suddenly changes.

2. Three-phase voltage PWM rectifier

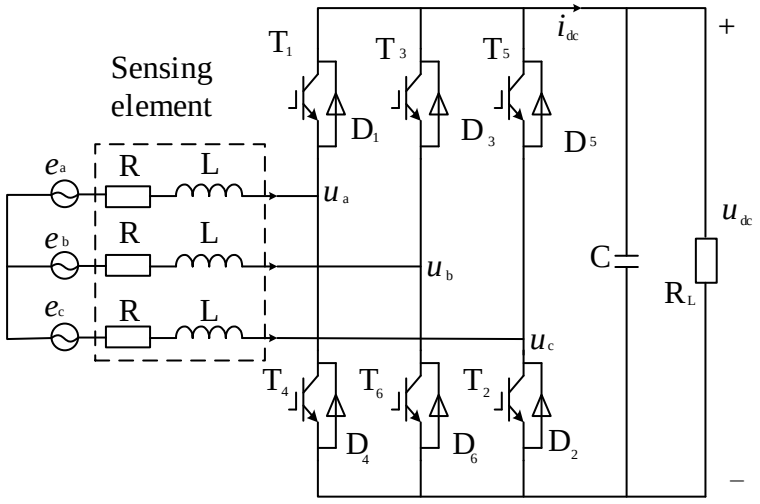

Figure 1. Topology of three phase voltage source PWM rectifier

Figure 1 is the main circuit topology of the three-phase voltage PWM rectifier [9], where e_a、e_b、 e_c are three-phase grid electromotive force, i_a、 i_b、i_c are three-phase grid current, u_{dc} and idc are DC bus voltage and current, ua, ub, uc are network side voltages, three-phase inductor L can not only filter but also have a boost effect, DC side capacitor C can filter and is voltage stable. The voltage-current equation of the rectifier and the conversion equation under the coordinates of α-β are:

$$\begin{cases} \begin{bmatrix} e_a \\ e_b \\ e_c \end{bmatrix} = R\begin{bmatrix} i_a \\ i_b \\ i_c \end{bmatrix} + L\frac{d}{d_t}\begin{bmatrix} i_a \\ i_b \\ i_c \end{bmatrix} + \begin{bmatrix} u_a \\ u_b \\ u_c \end{bmatrix} \\ C\dfrac{du_{dc}}{dt} = S_a i_a + S_b i_b + S_c i_c - i_{dc} \end{cases} \tag{1}$$

$$\begin{bmatrix} x_a \\ x_b \end{bmatrix} = \frac{2}{3}\begin{bmatrix} 1 & -1/2 & -1/2 \\ 0 & \sqrt{3}/2 & -\sqrt{3}/2 \end{bmatrix} \tag{2}$$

3. Traditional direct power control

Direct power control (DPC) is to multiply the instantaneous output voltage as the voltage outer loop by the current to obtain a given value of the instantaneous active power [10-11], compare the difference between the instantaneous P and transient Q at the input and the given power values P^* and Q_*, send the difference to the hysteresis comparator, and finally select the desired switch modulation signal in the switching state table through the switching signals S_p、 S_q, and the sector signal θ_n.

definition:

$$\begin{cases}\Delta P = P - P^* \\ \Delta Q = Q - Q^*\end{cases} \quad 3)$$

ΔP: The difference between a given active power P* and the actual measured active power P.

ΔQ: The difference between a given reactive power Q* and the actual measured reactive power Q.

If ΔP <0, the switching action reduces the instantaneous active power Q; conversely, the P increases.

If ΔP <0, the switching action reduces the instantaneous reactive power Q; conversely, the Q increases.

The three-phase voltage rectifier circuit operates in the traditional DPC mode, no matter what time point, the switch tubes on the bridge arm are in different on states in turn, and the number of switch tubes that can be turned on is 3. Therefore, the 8 input voltage vectors in the rectifier circuit are corresponding to the 8 combinations of switching states generated by the circuit, which are:

$$U_0(000), U_1(001), U_2(110), U_3(010), U_4(011), U_5(001), U_6(101), U_7(111)$$

Among them, U0 and U7 are called zero vectors, because in these two states there is no energy exchange between the two sides of the rectifier, and the rest of U1 to U6 are called non-zero vectors. This article refers to the eight input vectors of U0 to U7 as basic space vectors. The switching status is shown in Table 1.

Table 1. Eight switching states of the circuit

Number	1	2	3	4	5	6	7	8
switch state S_a S_b S_c	001	010	011	100	101	110	111	000
Conduction	$VT_4(D_4)$ $VT_6(D_6)$ $VT_5(D_5)$	$VT_4(D_4)$ $VT_3(D_3)$ $VT_2(D_2)$	$VT_4(D_4)$ $VT_3(D_3)$ $VT_5(D_5)$	$VT_1(D_1)$ $VT_6(D_6)$ $VT_2(D_2)$	$VT_1(D_1)$ $VT_6(D_6)$ $VT_5(D_5)$	$VT_1(D_1)$ $VT_3(D_3)$ $VT_2(D_2)$	$VT_1(D_1)$ $VT_3(D_3)$ $VT_5(D_5)$	$VT_4(D_4)$ $VT_6(D_6)$ $VT_2(D_4)$

Traditional direct power control is achieved through a logic switching meter, but at the same time affected by a switching meter control, which not only causes significant fluctuations in DC voltage and power when the load changes, but also degrades the performance of the rectifier.

4. Virtual magnetic chains

Because the circuit structure of the AC side of the rectifier is similar to the equivalent circuit of an AC motor, the power supply on the grid side can generally be regarded as a virtual AC motor. In order to reduce the sensing components on the AC side of the grid, to facilitate the estimation of instantaneous power, in addition, considering that the electric potential of the distribution network is generated by blocking the rotating magnetic field generated by the three-phase winding, thus leading to the concept of virtual magnetic chains.

According to the definition of the virtual magnetic chain Ψ=∫edt, the α-β axis component of the virtual magnetic chain is obtained:

$$\begin{cases} \Psi_a = \int e_\alpha \, dt = \int \left(L \dfrac{dt_\alpha}{dt} + R i_\alpha + u_\alpha \right) dt \\ \Psi_b = \int e_\beta \, dt = \int \left(L \dfrac{dt_\beta}{dt} + R i_\beta + u_\beta \right) dt \end{cases} \tag{4}$$

Improvements are made on the traditional virtual flux, and a first-order low-pass filter is commonly used to replace its pure integration region to eliminate DC bias and higher harmonics, and to suppress global integration saturation and estimate the virtual flux.

Given that the transfer function of the first-order low-pass filter is G(s), the expression for the new virtual flux Ψ is:

$$\Psi(s) = G(s) \cdot u(s) = \frac{1}{s + \omega_c} u(s) \tag{5}$$

s: Laplace transform complex variable from time domain to complex domain transfer function, u(s): input quantity, Ψ(s): output amount, ωc: cutoff frequency.

Fundamentally, a first-order low-pass filter is equivalent to a pure integrator in series with a first-order high-pass filter. The transfer function of a pure integrator is:

$$G(s) = \frac{1}{s} \tag{6}$$

Assuming that a sampled signal can be described as Udc+ Aωsin(ωt), its time-domain response through a pure integrator and a first-order low-pass filter is shown in Fig. 2.

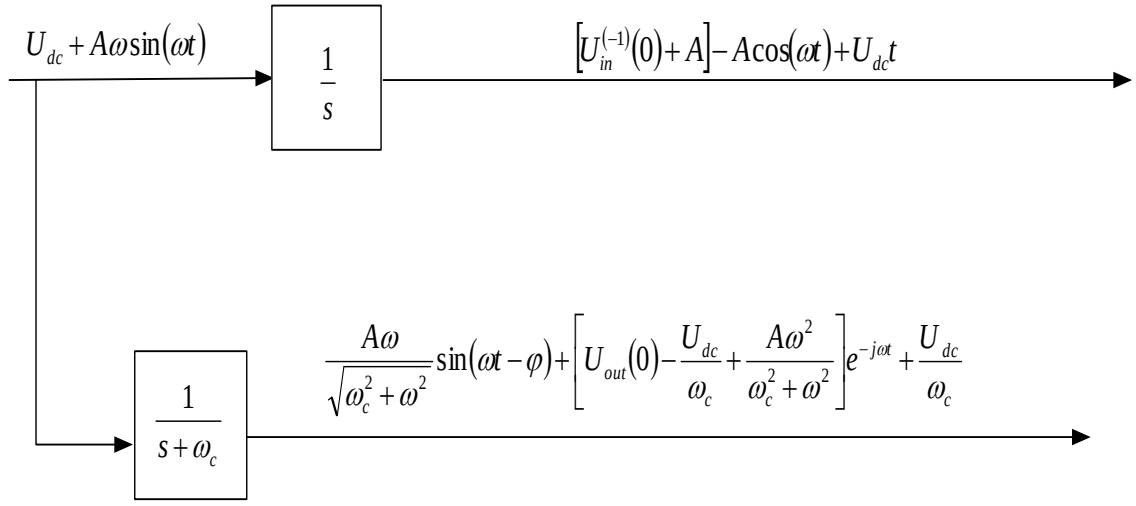

Figure 2. Time domain response of pure integrator and first-order low-pass filter

In Figure 2, Udc represents the DC offset of the sampled signal; ω is the angular frequency of the grid fundamental frequency signal; Uin(-1)(0) is the integration value of the input signal at 0 moment; and Uout(0) is the initial output value of the first-order low-pass filter.

The initial value problem and integral drift of the pure integrator can be seen from the analytical expression of the output signal in Figure 2, and the DC attenuation effect of the first-order low-pass filter cutoff frequency ωc can also be observed. Substitute s = jω into (5) and (6) to get:

$$\begin{cases} G_1(j\omega) = \dfrac{1}{j\omega + \omega_c} = \dfrac{1}{\sqrt{\omega^2 + \omega_c^2}} e^{-jarctan\frac{\omega}{\omega_c}} \\ G(j\omega) = \dfrac{1}{\omega} e^{-j\frac{\pi}{2}} \end{cases} \tag{7}$$

Comparing the two equations in (7), it can be seen that since the ωc in the actual system is not 0, this method still brings the problem of amplitude and phase error. Aiming at the difference in amplitude and phase frequency characteristics between the first-order low-pass filter and the pure integral, an improved method is proposed.

5. Cross-compensated virtual magnetic chains

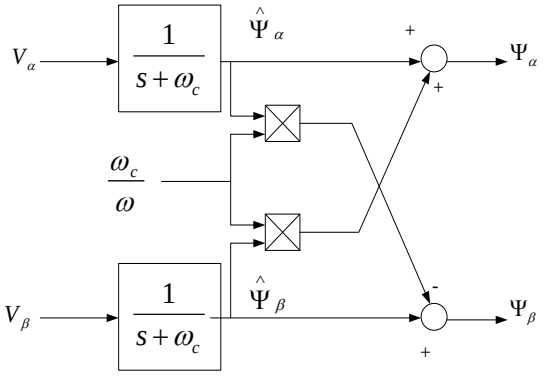

Figure 3. Cross-compensated low-pass filter

When using a first-order low-pass filter to estimate the grid virtual flux, the relationship between the grid voltage vector and the estimated virtual flux vector is as follows:

$$\hat{\Psi} = \frac{\hat{V}}{(j\omega + \omega_c)} \tag{8}$$

where Ψ represents the estimated virtual flux vector. Equation (8) can also be written as:

$$\hat{\Psi} = \frac{\hat{V}}{\omega_c^2 + \omega^2}(\omega_c - j\omega) \tag{9}$$

Substitute the correlation formula Ψ=V/jw Ψ=V/jw of voltage vector and virtual flux vector into (9) to obtain:

$$\hat{\Psi} = \frac{\hat{V}}{\omega_c^2 + \omega^2}\omega(\omega + j\omega_c) \tag{10}$$

So:

$$\frac{\hat{\Psi}}{\Psi} = \frac{\hat{\Psi}}{\Psi}\angle\hat{\theta} - \theta = \frac{\omega}{\sqrt{\omega^2 + {\omega_c}^2}}\angle\varphi \tag{11}$$

where Ψ represents the corresponding estimate of the amplitude of the actual flux vector Ψ; θ represents the corresponding estimate of the phase θ of the actual flux vector.

The α components of the actual flux vector can be written as:

$$\Psi_\alpha = \Psi\cos\left(\hat{\theta} - \varphi\right) = \Psi_\alpha + \Psi_\beta\frac{\omega_c}{\omega} \tag{12}$$

Similarly, the β component is obtained as:

$$\Psi_\beta = \Psi_\beta - \Psi_\alpha\frac{\omega_c}{\omega} \tag{13}$$

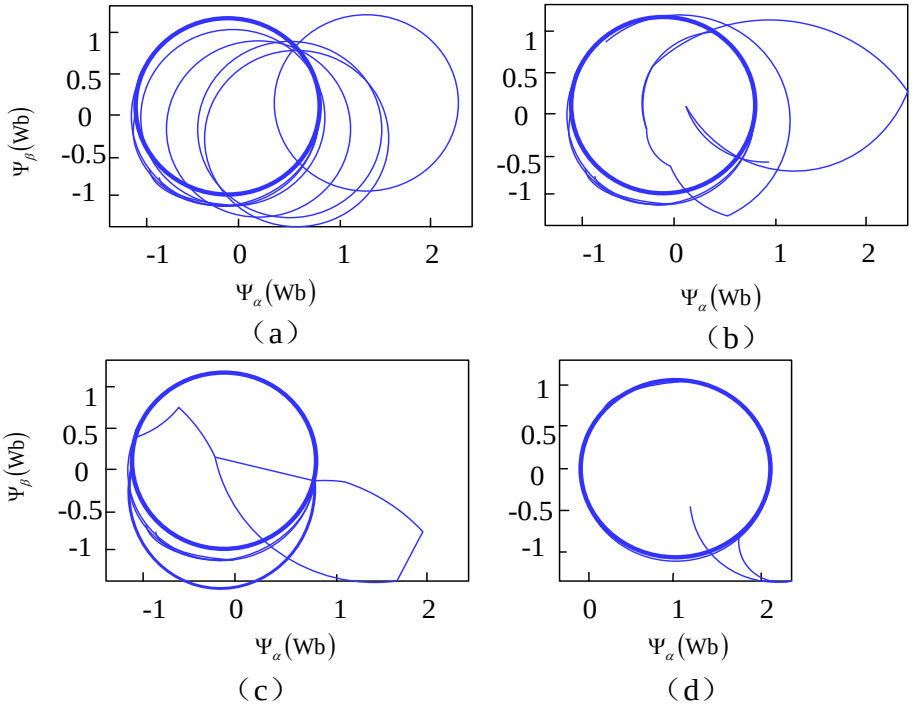

Figure 4. Comparison of pure integrators with parallel compensated observers

Parallel low-pass virtual flux observer observations are shown in Figure 2.6. Figure 4 takes the cutoff frequency ω_c = 30,100,500,1000, respectively. Comparing the observations of the cutoff frequency in the above four values, it is known that the speed at which the virtual flux observation reaches the steady state increases as the cutoff frequency increases, but further simulation studies show that it is not that the larger the cutoff frequency, the better. At the same time, there is no DC offset problem in the virtual flux observation based on the parallel compensation observer.

6. Cross-compensated virtual magnetic chain double switch table DPC

Figure 5 shows a three-phase PWM rectifier virtual flux double switch table DPC block diagram. The virtual flux principle is introduced on the AC side, and the difference between the given value of instantaneous active power and reactive power and the actual

measured instantaneous power value is controlled by selecting the appropriate switching signal through the hysteresis comparator to control the opening and closing of the switch tube. In the figure, two switching tables are used to control P and Q separately to improve the problem of large fluctuations and instability of the DC bus voltage.

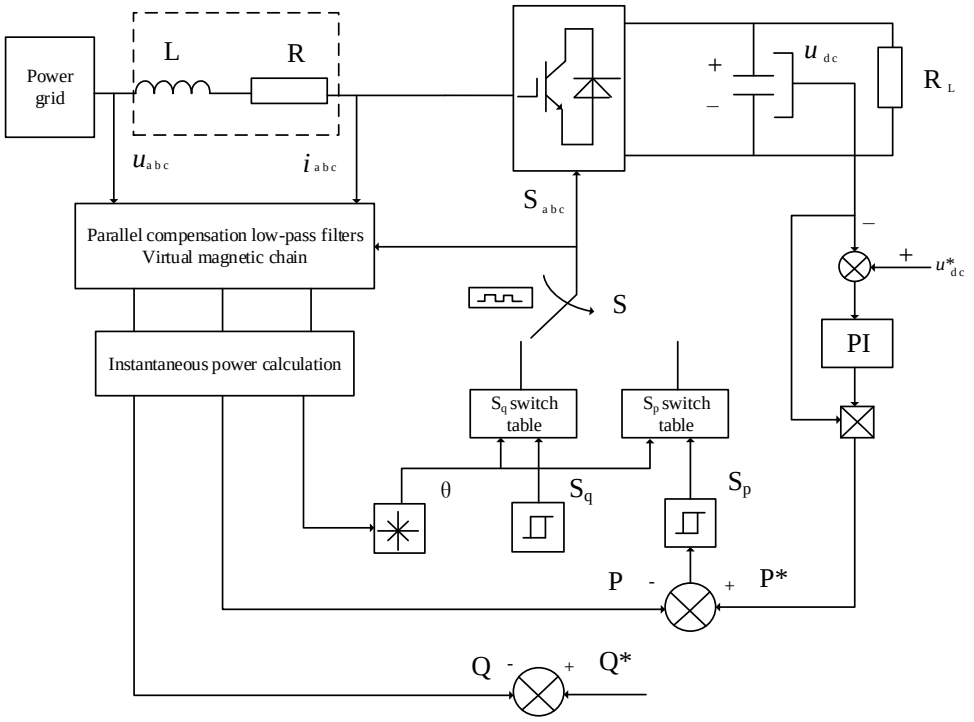

Figure 5. Parallel compensation virtual magnetic chain double switch table DPC block diagram

6.1 New Switch Status Table

The three-phase voltage rectifier circuit runs in the traditional DPC mode, no matter what time point, the switch tube on one bridge arm corresponds to only one conduction state, so there are three switch tubes on the three bridge arms that can be turned on. Then in the rectifier circuit, 8 switching state combinations can be generated, which correspond to 8 input voltage vectors, namely U0 (000), U1 (100), U2 (110), U3 (010), U4 (011), U5 (001), U6 (101), U7 (111). Traditional direct power control is achieved through a logic switching meter, but at the same time affected by a switching meter control, which not only causes significant fluctuations in DC voltage and power when the load changes, but also degrades the performance of the rectifier. In order to reduce power ripple and control power more flexibly, the entire space can be divided into 12 sectors to optimize the input voltage vector of the three-phase voltage rectifier circuit, and a logic switch table can be changed to two switch tables to control P and Q respectively, and the optimized switch table can improve the power

regulation performance of the rectifier. Figure 6 shows the 12 sector space vector diagram, and Table 2 shows the switching table of the power supply voltage vector in 12 sectors.

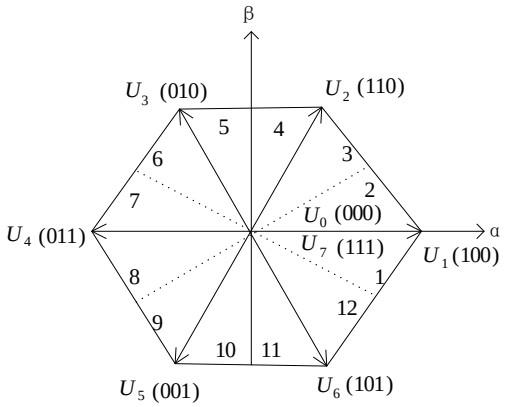

Figure 6. Space vector diagram of 12 sectors

Table 2. Double on off table of power supply voltage vector in 12sectors

S_p	θ_1	θ_2	θ_3	θ_4	θ_5	θ_6	θ_7	θ_8	θ_9	θ_{10}	θ_{11}	θ_{12}
0	U_1	U_1	U_2	U_2	U_3	U_3	U_4	U_4	U_5	U_5	U_6	U_6
1	U_4	U_4	U_5	U_5	U_6	U_6	U_1	U_1	U_2	U_2	U_3	U_3
S_q	θ_1	θ_2	θ_3	θ_4	θ_5	θ_6	θ_7	θ_8	θ_9	θ_{10}	θ_{11}	θ_{12}
0	U_6	U_6	U_1	U_1	U_2	U_2	U_3	U_3	U_4	U_4	U_5	U_5
1	U_2	U_2	U_3	U_3	U_4	U_4	U_5	U_5	U_6	U_6	U_1	U_1

Thereinto:

$$\begin{cases} \dfrac{(n-1)\pi}{6} \le \theta_n \le \dfrac{n\pi}{6} \\ \theta = arctan\dfrac{u_\beta}{u_\alpha} \\ n = 1,2,3 \dots 12 \end{cases} \tag{14}$$

The logical switch function is:

$$S_p \begin{cases} 0, \Delta p < H_p \\ 1, \Delta p \ge H_p \end{cases}, \quad S_q \begin{cases} 0, \Delta q < H_q \\ 1, \Delta q \ge H_q \end{cases} \tag{15}$$

6.2 Cross-compensated virtual flux DPC

When the intermediate connection reactor equivalent resistor R is ignored, the AC side voltage equation for the three-phase voltage source converter is:

$$V = U + L\frac{dI}{dt} \tag{16}$$

The two sides of the equal sign are integrals:

$$\Psi = \Psi_U + LI \tag{17}$$

Where Ψu represents the virtual flux vector at the converter end. Then the calculation of Ψu in the coordinate system of α−β is as follows:

$$\begin{aligned} \Psi_{u\alpha} &= \int \left\{ \sqrt{\frac{2}{3}} V_{dc} \left[S_a - \frac{1}{2}(S_b + S_c) \right] \right\} dt \\ \Psi_{u\beta} &= \left[\sqrt{\frac{1}{2}} V_{dc}(S_b - S_c) \right] dt \end{aligned} \tag{18}$$

Therefore, using the integration operation in parallel compensated virtual flux implementation (16), the expression for the grid port virtual flux estimation of the three-phase voltage rectifier topology is as follows:

$$\begin{aligned} \Psi_\alpha &= \hat{\Psi}_{u\alpha} + \hat{\Psi}_{u\beta}\frac{\omega_c}{\omega} + LI_\alpha \\ \Psi_\beta &= \hat{\Psi}_{u\beta} + \hat{\Psi}_{u\alpha}\frac{\omega_c}{\omega} + LI_\beta \end{aligned} \tag{19}$$

The grid vector is:

$$\mathrm{V} = \frac{\mathrm{d}\Psi}{\mathrm{dt}} = \frac{\mathrm{d}\left(\Psi \mathrm{e}^{\mathrm{j}\omega \mathrm{t}}\right)}{\mathrm{dt}} = \frac{\mathrm{d}\Psi}{\mathrm{dt}}\mathrm{e}^{\mathrm{j}\omega \mathrm{t}} + \mathrm{j}\omega\Psi \tag{20}$$

The instantaneous power on the α-β coordinate system is:

$$\begin{cases} \mathrm{P} = \mathrm{Re}(\mathrm{VI}^*) = \left.\dfrac{\mathrm{d}\Psi}{\mathrm{dt}}\right|_\alpha \mathrm{I}_\alpha + \left.\dfrac{\mathrm{d}\Psi}{\mathrm{dt}}\right|_\beta \mathrm{I}_\beta + \omega\left(\Psi_\alpha \mathrm{I}_\beta - \Psi_\beta \mathrm{I}_\alpha\right) \\ \mathrm{P} = \mathrm{Im}(\mathrm{VI}^*) = -\left.\dfrac{\mathrm{d}\Psi}{\mathrm{dt}}\right|_\alpha \mathrm{I}_\alpha + \left.\dfrac{\mathrm{d}\Psi}{\mathrm{dt}}\right|_\beta \mathrm{I}_\beta + \omega\left(\Psi_\alpha \mathrm{I}_\beta + \Psi_\beta \mathrm{I}_\alpha\right) \end{cases} \tag{21}$$

When the grid voltage is sinusoidal, then the virtual flux voltage vector amplitude is unchanged, that is, the microsonance of the flux amplitude is 0. Thus (21) may be reduced to:

$$\begin{cases} P = \omega\left(\Psi_\alpha I_\beta - \Psi_\beta I_\alpha\right) \\ Q = \omega\left(\Psi_\alpha I_\alpha - \Psi_\beta I_\beta\right) \end{cases} \tag{22}$$

7. Simulation and experimental verification

7.1 Simulation verification

The direct power control of the virtual flux double-switch table of the three-phase voltage rectifier proposed in this paper and the traditional direct power control are simulated to verify the effectiveness of the DPC control method proposed in this paper. Table 3 shows the simulation parameters for the design.

Table 3. Simulation parameters

variable	numeric value
DC bus voltage U_{dc}	700V
Three-phase AC line voltage peak Um	380V
Voltage frequency f	60Hz
Filter inductor L	200mH
Line resistance R	0.6Ω
Equivalent payload R_L	100Ω
DC side capacitor C	5100μF
Simulation time t	1s
Load mutation time t_0	0.5s

According to the parameters in Table 3, the instantaneous active power and reactive power output of the rectifier are simulated by the traditional DPC method and the cross-compensated virtual flux DPC strategy, respectively, and the results are shown in Figure 7. The left and right figures are simulated waveforms of active power and reactive power under the traditional DPC and cross-compensated virtual flux DPC strategies, respectively. From the figure, it can be found that whether before the load mutation or after the load mutation, the active power is from 5000 mutation to 10000W, but the active power waveform of the right figure is smoother and more stable, while the glitch after the reactive power mutation

under the traditional DPC is in the range of 500Var, and the harmonic glitch brought by the latter is also within 200Var in time, making the reactive power more inclined to 0, and the harmonic content contained is significantly reduced.

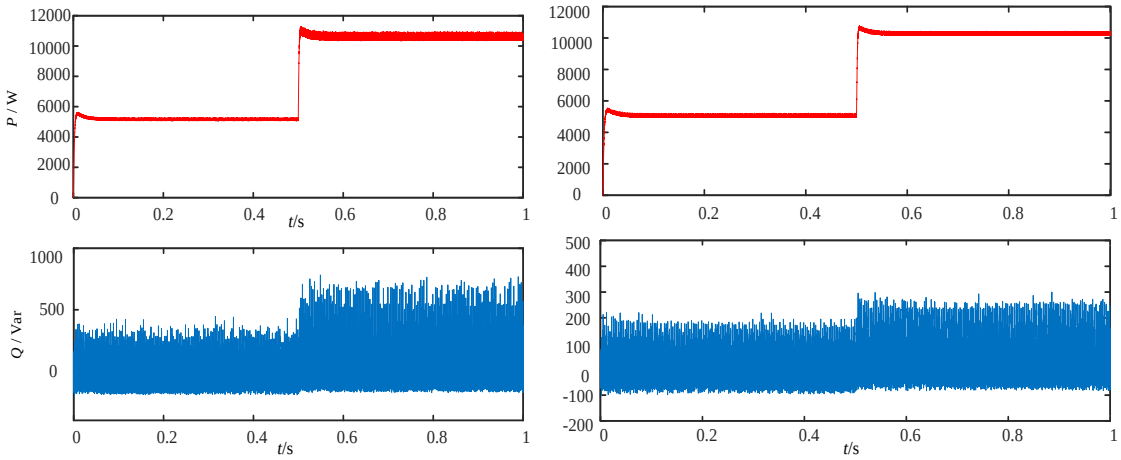

Figure 7. Active and reactive power comparison chart

The dc bus voltages of the two methods are compared and simulated, and the simulation waveform results are shown in Figure 8, where 1 is the DC bus waveform under the traditional DPC and 2 is the DC bus voltage waveform under the cross-compensating virtual flux DPC. It can be seen in the figure that the DC bus voltage of the new DPC can not only be quickly tracked to a given value after a 0.5s load mutation, but also has good dynamic performance, but also inhibits the pulsation after the mutation, so that the ripple is very small. After the load sudden change, the AC side voltage and current can also be quickly stabilized at the reference value.

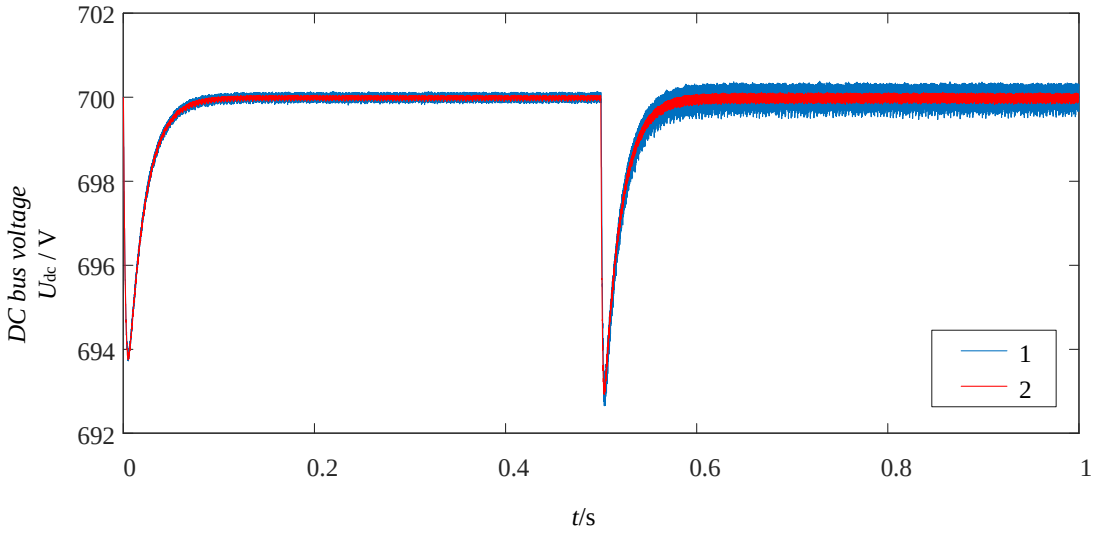

Figure 8. DC bus voltage comparison waveform

Figure 9 is a comparison of the harmonic content of the traditional DPC and the cross-compensating virtual magnetic chain, in the figure a is the harmonic content curve of the traditional DPC, and b is the harmonic content curve of the cross-compensated virtual magnetic chain double-switch table DPC. For the harmonic analysis of the current of the rectifier network side phase A, the THD=8.43% when the traditional DPC control is adopted, and the THD=3.42% after the new DPC control is adopted, which is significantly reduced, which effectively improves the current quality of the grid side.

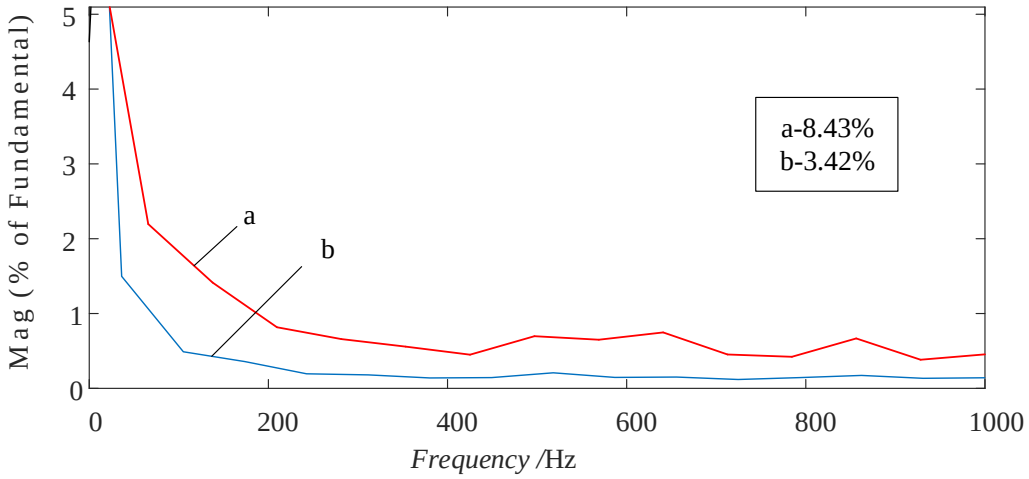

Figure 9. Comparison chart of harmonic content

7.2 Experimental Verification

In the school's power electronics laboratory, an experimental bench was built to conduct experiments on the three-phase voltage rectifier circuit. In the experiment, the voltage on the grid side is 380V, the DC voltage is 700V, the load is selected with 100Ω resistor, the control chip is selected from TI's TMS320F2812, and the switching device is selected from Fujifilm's IGBT-IPM module 7MBP100RA120. Figure 10 shows a voltage and current waveform diagram of the AC side of the cross-compensated virtual magnetic chain DPC. The voltage and current waveforms on the grid side are sine waveforms with smooth waveforms. Figure 11 shows the TTL spectrum comparison plot, where a is the TTL spectrum distribution of the traditional DPC, and b is the TTL spectrum distribution under the cross-compensated virtual flux double-switch table DPC. It can be seen from the figure that the harmonic distribution of the cross-compensated virtual flux DPC is significantly reduced.

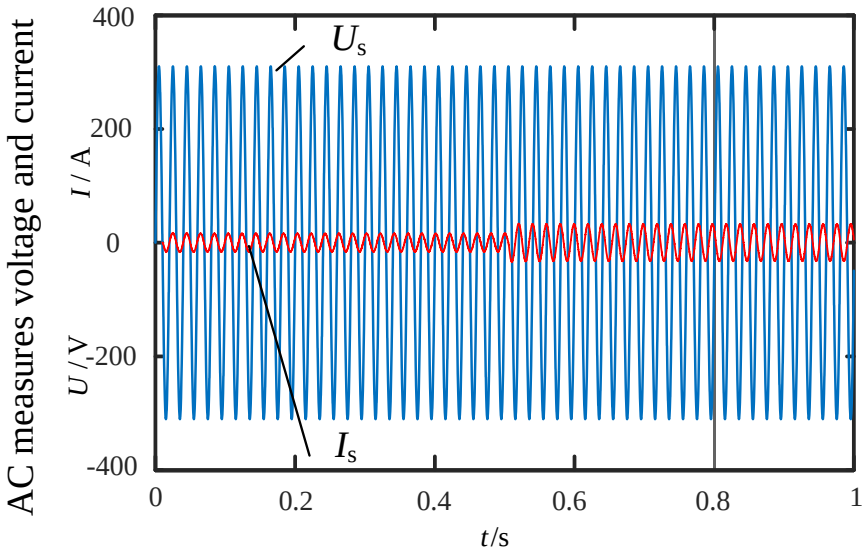

Figure 10. Voltage and current waveform of AC side

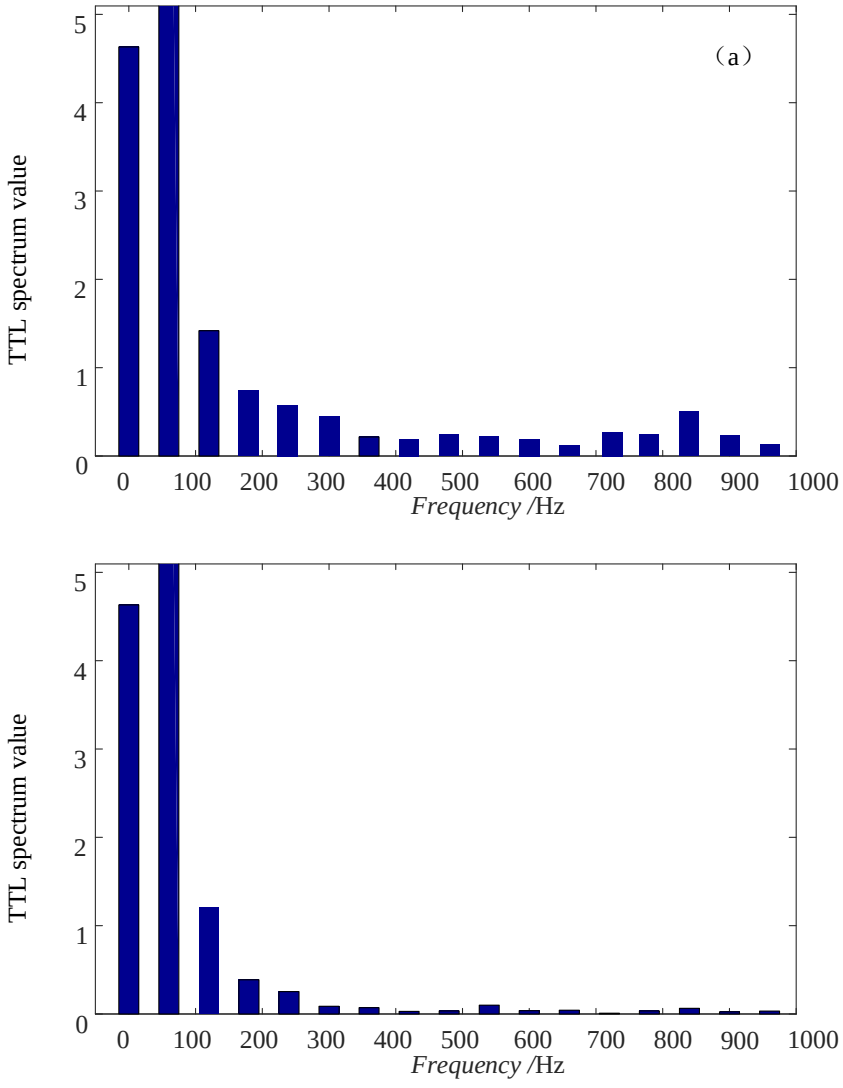

Figure 11. TTL spectrum comparison diagram

8. Conclusion

The direct power control strategy of the three-phase voltage PWM rectifier circuit virtual flux double-switch meter proposed in this paper, reasonably reduces the use of components by adding a cross-compensated virtual magnetic chain on the power grid side, and subdivides the switching status table sector and switches to the dual-switch meter to control the power. The simulation and experimental verification of the traditional virtual magnetic chain DPC and the proposed new virtual magnetic chain double-switch table DPC were carried out, and the experimental results showed that the proposed DPC can more smoothly control the instantaneous active power P and reactive power Q, so that the reactive power tends to 0, the power ripple is smaller, even after the mutation, it can quickly tend to be stable, the waveform is stable, and the harmonic content is significantly reduced compared with the traditional DPC control, which has better robustness.

References

[1] Zheng Zhongjiu. Control strategy and application of three-phase voltage PWM rectifier[D]. Dalian: Dalian University of Technology, 2011: 1-2.

[2] Zheng Zheng, Wang Yingqiu. Voltage chullum control strategy of cascaded H-bridge rectifier circuit[J].Power Electronics Technology,2016,50(5):76-79.

[3] Gan Xue. Research on on-board charging power supply of electric vehicle[D].Sichuan: Xihua University, 2018:13-14.

[4] Feng Zewen. Research on direct power control strategy based on PWM rectifier[J].Communication Power Supply Technology,2020,37(7): 231-233

[5] Ren Haifeng, Liu Shuxi, Su Xinzhu, etc. Virtual Flux-Oriented Three-Phase Voltage Source Pulse Width Modulation Rectifier Model Predicts Direct Power Control[J].Journal of Chongqing Electric Power College,2021,26(2): 2-4.

[6] M Malinowski,M P Kazmierkowski,S Hansen,et al. Virtual Flux Based Direct Power Control of Three-phase PWM Rectifier.[J].IEEE Trans.on Ind. Applications,37(4):1019-1027.

[7] Zhang Yi,Li Z, Zhang Y, et al. Performance Improvement of Direct Power Control of PWM Rectifier With Simple Calculation.[J].IEEE Trans.on Power Electronics,2013,28(7): 3428-3437.

[8] Huang Shoudao, Ye Hongzhi, Zhang Wenjuan, et al. Application of Direct Power Control Based on Virtual Flux in VSC-HVDC[J].Power Grid Technology.2014,38(4): 852-857.

[9] Lin Weixun. Modern power electronics technology[M]. Beijing:China Machine

Press.2018:326-328.

[10] Gao Xin, Sun Fayi. Three-phase voltage type PWM rectifier direct power control system[J].Heilongjiang Science and Technology Information, 2016:29.

[11] Liao Zhiling, Cui Qinghua. Variable coefficient frequency reduction model predicts direct power control[J]. Electronic Devices, 2018, 41(06):1 416-1421.

[12] Feng Zewen. Research on Direct Power Control Strategy Based on PWM Rectifier[J].Communication Power Supply Technology,2020,37(7):231-233.

Author's biography

He Liu, Bachelor of power electronics and electric drives. Now studying Master of Information and Information Processing Theory and Application at Liaoning University of Technology majoring in the Department of Electronics and Communication Engineering, and currently engaged in research on fake reviews detection and rectifier designs.

Wang Ya-jun, Professor, Ph.D, is engaged in research related to power electronic technology and application, modern power supply technology, signal and information processing